LEVEL

ARE 13095.3-P

RESEARCH ON RESONANT CHARGE-EXCHANGE
X-RAY AND ULTRAVIOLET LASERS

Final Report

Grant No. DAHC04-75-G-0193
Grant No. DAAG29-77-G-0134

DDC

APR 12 1979

C

Prepared by

William B. McKnight

March 1979

The University of Alabama in Huntsville
Department of Physics
Huntsville, Alabama 35807

79 04 09 023

RESEARCH ON RESONANT CHARGE-EXCHANGE
X-RAY AND ULTRAVIOLET LASERS
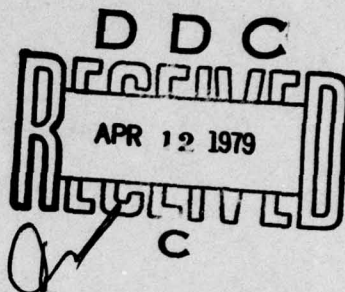
Final Report

Grant No. DAHC04-75-G-0193
Grant No. DAAG29-77-G-0134

Prepared by

William B. McKnight

March 1979

The University of Alabama in Huntsville
Department of Physics
Huntsville, Alabama 35807

REPORT DOCUMENTATION PAGE	READ INSTRUCTIONS BEFORE COMPLETING FORM

1. REPORT NUMBER (18) ARO (19) 13095.3-P	2. GOVT ACCESSION NO.	3. RECIPIENT'S CATALOG NUMBER

4. TITLE (and Subtitle)

RESEARCH ON RESONANT CHARGE-EXCHANGE X-RAY AND ULTRAVIOLET LASERS.

5. TYPE OF REPORT & PERIOD COVERED

Final Report. 16 Jun 75 - 28 Dec 79
6/16/75 - 12/28/79

6. PERFORMING ORG. REPORT NUMBER

7. AUTHOR(s)

(10) William B. McKnight

8. CONTRACT OR GRANT NUMBER(s)

(15) DAHC04-75-G-0193
DAAG29-77-G-0134

9. PERFORMING ORGANIZATION NAME AND ADDRESS

The University of Alabama in Huntsville
Department of Physics
Huntsville, Alabama 35807

10. PROGRAM ELEMENT, PROJECT, TASK AREA & WORK UNIT NUMBERS

11. CONTROLLING OFFICE NAME AND ADDRESS

U. S. Army Research Office
P. O. Box 12211
Research Triangle Park, NC 27709

12. REPORT DATE

March 1979

13. NUMBER OF PAGES

17 (12) 22p.

14. MONITORING AGENCY NAME & ADDRESS(if different from Controlling Office)

15. SECURITY CLASS. (of this report)

Unclassified

15a. DECLASSIFICATION/DOWNGRADING SCHEDULE

16. DISTRIBUTION STATEMENT (of this Report)

Approved for public release; distribution unlimited

17. DISTRIBUTION STATEMENT (of the abstract entered in Block 20, if different from Report)

NA

18. SUPPLEMENTARY NOTES

The findings in this report are not to be construed as an official Department of the Army position, unless so designated by other authorized documents.

19. KEY WORDS (Continue on reverse side if necessary and identify by block number)

Lasers, X-rays, ultraviolet, charge-exchange, plasmas

20. ABSTRACT (Continue on reverse side if necessary and identify by block number)

This report presents a summary of work carried out on x-ray and far ultraviolet laser research, in which excited states are obtained by charge-exchange between an atom or ion and a fully stripped ion. Schemes investigated include the expansion of plasma produced in a shock-tube and a plasma produced by a laser-target interaction. The laser-produced plasma, intended to produce stimulated emission at 132 Å, was the subject of experimental work, with negative results.

408 834

DD FORM 1473 EDITION OF 1 NOV 65 IS OBSOLETE
S/N 0102-014-6601

The findings in this report are not to be construed as an official
Department of the Army position, unless so designated by other
authorized documents.

TABLE OF CONTENTS

I. INTRODUCTION

This report covers the research performed under Grants DAHC04-75-G-0193 and DAAG29-77-G-0134 during the period June 16, 1975 to February 28, 1979. The goal of this research was to obtain stimulated emission at very short wavelengths (x-ray or far ultraviolet) by the use of charge-exchange reactions. Obtaining laser action at any short wavelengths has been a problem of great interest in the scientific community for some time, and the concept contained in the original proposal was believed to offer great promise for laser action at wavelengths below 1000 Å.

Many of the obstacles to obtaining laser action at x-ray and far ultraviolet wavelengths appear to be overcome by completely stripping atoms and then adding one electron to the ion through a charge-exchange reaction to form an atom (hydrogenic, if the ion was fully stripped) that could radiate at very short wavelengths. By choosing the neutral atom properly the charge-exchange reaction can be made to have a very large cross-section-10^{-15}cm^2 or larger. If the additional electron is in an outer shell the ion cannot decay through the very fast Auger transitions and a useful lifetime in the excited state may be achieved.

This work was begun based on a proposed scheme to use an ion beam of alpha particles and to interact the beam with hydrogen target atoms to obtain charge-exchange and a helium ion in the 2p state from which it radiates to the 1s state.

$$He^{++} + H_{1s} \rightarrow He^+_{2p} + H^+ \rightarrow He^+_{1s} + \gamma(304 \text{ Å}) + H^+$$
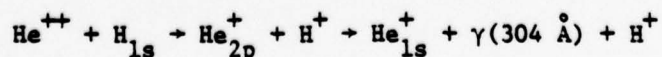
As there are no ground state ions in the system this would be expected to yield an inversion. It was planned to perform the experiment at

Los Alamos in a joint program with the University of Arizona and Los
Alamos Scientific Laboratory. However, sometime after this research
began, the program was terminated for non-technical reasons.

II. SUMMARY OF RESULTS

Several systems for obtaining inversions at very short wave-
lengths by charge-exchange were investigated, and as the charge-exchange
reaction appeared to be the best candidate, several possibilities were
analyzed. Plasmas as the source of the ions were analyzed and a system
devised to use a shock tube for generating a plasma, with charge-ex-
change occurring after expansion through a nozzle. This system is out-
lined in Appendix I and two specific cases, hydrogenic helium (lasing
at 1640 Å) and lithium (729 Å) were considered in some detail.

Another arrangement, using a laser-produced plasma, is described
in Appendix II. This uses a plasma formed by the interaction of a
high-power laser with a carbon target to yield fully stripped C VII.
If the streaming velocity of the carbon ions is then of the order of
3×10^7 cm/sec, preliminary calculations indicated the cross section
for the pickup of an electron by the carbon into the n = 3 state, that
is the charge exchange reaction

$$C^{+6} + Ar^{+2} \rightarrow C^{+5}(n = 3) + Ar^{+3}$$
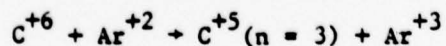
is of the order of 10^{-15} cm^2. The carbon ion then radiated the Balmer-α
line at 182 Å. According to the analysis a 1 cm diameter Nd-glass laser
with an output of 30 joules in a pulse duration of 10 nanoseconds,
focused by a cylindrical lens would yield significant gain.

As it appeared feasible to experimentally investigate the C VII -
Ar III system, this was chosen for experimental work. Two short-pulse
ruby oscillator-amplifier systems, designed to be fired sequentially
in a master-slave arrangement were borrowed from MIRADCOM. The Space
Sciences Laboratory of the Marshall Space Flight Center, NASA, offered
the use of a grazing-incidence McPherson monochromator, which was
capable of being differentially-pumped across an open slit and could
be used in the region around 182 Å. The ruby lasers were limited to
about 11 joules output in order to avoid damage to the amplifier ruby
rods. Their pulse durations were measured by a photodiode to be of
the order of 15-20 nanoseconds, and consequently, lacked the peak power
capability to reach the conditions outlined in Appendix II. The lasers
were repaired and modified so that they could be Q-switched simultaneously
(within a few nanoseconds) by switching both Pockels cells with a
single thyratron and adjusting the lead lengths appropriately. It was
planned by this method to use a two-plasma technique in which the 182 Å
Balmer-α line would be observed for gain between the firing of one
laser and subsequent firing of both lasers simultaneously.

An interaction cell was fabricated with provision for a target,
focussing lens, background gas pressure control, and positioning of
the target with respect to the monochromator slit.

Numerous shots were carried out with a single laser in order to
find line radiation at 182 Å which could be attributable to charge-
exchange. The ruby laser was operated at about 5 joules output to
avoid destruction of the flashlamps. Strong signals were obtained from
the plasma at 182 Å but also at neighboring wavelengths, indicating

that line radiation was not being obtained. These signals were obtained both with and without a background gas and indicate that the radiation observed was not due to charge-exchange. Measurements of the plasma front velocity indicated ion streaming velocities in the range from 5×10^6 cm/sec to 1.5×10^7 cm/sec, being slower with increased background gas pressure. As later calculations indicate that even at 3×10^7 cm/sec the cross-section for electron capture into the $n = 3$ state is only 2×10^{17} cm^2 it appears that at the ion streaming velocities obtained in the experiment, the electron-capture cross section into the $n = 3$ state is much too low for charge-exchange to generate a significant inversion on the Balmer-α line of C VI under these conditions.

III. LIST OF PUBLICATIONS

1. William B. McKnight and John F. Seely: "Lasing on the Balmer-α
    Line of Shock Tube Generated Plasma Ions" [Opt. Commun. 21, 247
    (1977)].

2. John F. Seely and William B. McKnight: "Soft X-Ray Laser Pumped
    by Charge Exchange between C VII and Ar III in Expanding Laser-
    Produced Plasma" [J. Appl. Phys. 9, 3691 (1977)].

IV. LIST OF SCIENTIFIC PERSONNEL

The following persons assisted in the research under these grants:

W. B. MCKNIGHT, Research Professor of Physics, Principal Investigator

J. F. SEELY, Senior Research Associate

W. V. DENT, Graduate Research Assistant

T. R. PHILLIPS, Undergraduate Laboratory Assistant

D. R. HULSEY, Undergraduate Laboratory Assistant

No degrees awarded

LASING ON THE BALMER-α LINE OF SHOCK TUBE GENERATED PLASMA IONS*

William B. McKNIGHT and John F. SEELY
Department of Physics, The University of Alabama in Huntsville, Huntsville, Alabama 35807, USA

Lasing on the Balmer-α line of hydrogen-like ions is shown to be possible in a shock tube generated plasma. The specific cases of hydrogen-like helium (lasing at 1640 Å) and lithium (729 Å) are considered in detail.

1. Introduction

The Balmer-α transitions of hydrogen-like ions are particularly interesting from the viewpoint of developing short wavelength lasers. The scaling of wavelengths and transition rates with atomic number are, of course, precisely known, and the electron collisional ionization and recombination of hydrogen-like ions are easily treated.

We first consider the circumstances under which a plasma consisting of fully stripped ions may be generated in a high energy shock tube. Charge exchange pumping [1–9] of the laser transition occurs as the plasma expands into a gas composed of neutral atoms as shown in fig. 1. We consider processes which compete with the pump reaction and laser transition, such

as electron collisional ionization of the neutral target atoms and collisional depopulation of the upper laser state, and determine the conditions for lasing on the Balmer-α line of the hydrogen-like plasma ion.

In highly ionized plasma, the fractional ionization is determined by the competition between collisional
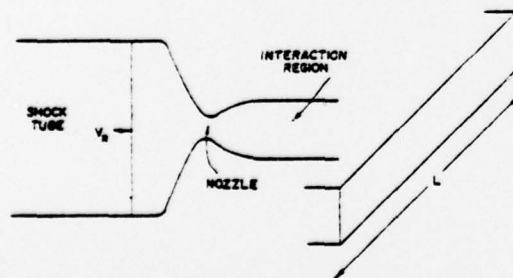

Fig. 1. The plasma behind the reflected shock wave expands through the nozzle and mixes with the target gas in the interaction region. The length of the active medium, and the approximate diameter of the shock tube, is L
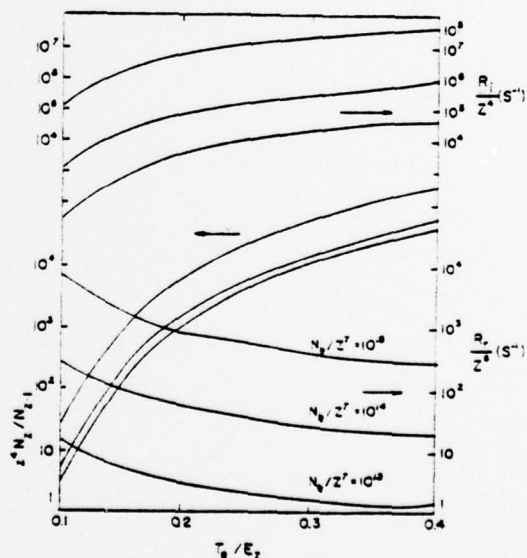
Fig. 2. The ionization rate R_i and recombination rate R_r as functions of the electron temperature T_e. The ratio of fully stripped ions to hydrogen-like ions is R_i/R_r. The lower curve in each group is for electron density $10^{13}Z^7$ cm^{-3}, the middle curve for $10^{14}Z^7$, and the upper curve for $10^{15}Z^7$. The ionization potential of the hydrogen-like ion is E_z. In steady state, the fractional ionization N_z/N_{z-1} is equal to R_i/R_r.

ionization and recombination. We are primarily inter-
ested in the densities of fully stripped and hydrogen-
like ions. For corona equilibrium [10], the rates of col-
lisional ionization R_i and radiative and three-body re-
combination R_r are shown in fig. 2, along with the
ratio of fully stripped ion density to hydrogen-like ion
density R_i/R_r. To obtain fully stripped ions with low
atomic number Z, the ratio of the plasma electron
temperature T_e to the ionization potential of the hydro-
gen-like ion E_z must be greater than 0.1–0.2. The frac-
tional ionization is a relatively weak function of N_e for
low electron density. For electron density greater than
$10^{16}Z^7$ cm^{-3}, Saha equilibrium prevails.

2. Shock generated plasma

A hot plasma may be generated behind a shock wave
propagating through a low density gas. Additional heat-
ing occurs when the primary shock wave is reflected
from the end of a shock tube. The temperature of the
plasma formed behind the primary shock wave may be
estimated by solving the conservation laws for mass,
momentum, and energy [11]:

$$N M (V - u) = N_0 M V, \qquad (1)$$

$$N M (V - u)^2 + P = N_0 M V^2 + P_0, \qquad (2)$$

$$\tfrac{1}{2} M (V - u)^2 + H = \tfrac{1}{2} M V^2 + H_0, \qquad (3)$$

where V is the velocity of the primary shock wave and
u is the flow velocity of the plasma behind the shock.
The density, pressure, and enthalpy ahead of the shock
are N_0, P_0, and H_0 respectively, and the corresponding
quantities behind the shock are N, P, and H. We make
the strong shock assumption $P \gg P_0$ and $H \gg H_0$. If the
plasma behind the shock is composed of fully stripped
ions in thermal equilibrium [12], then

$$P = k T N (1 + Z) \qquad (4)$$

$$H = \tfrac{1}{2} k T (1 + Z) + E_z. \qquad (5)$$

We may now solve for the plasma temperature as a func-
tion of shock velocity, and the results are shown in
fig. 3(a). To obtain fully stripped low-Z ions ($kT_e/E_z
\gtrsim 0.1$), the shock velocity must be greater than about
10^7 cm/s. Shock velocities of this magnitude are easily
obtained in high energy shock tubes [11]. The shock
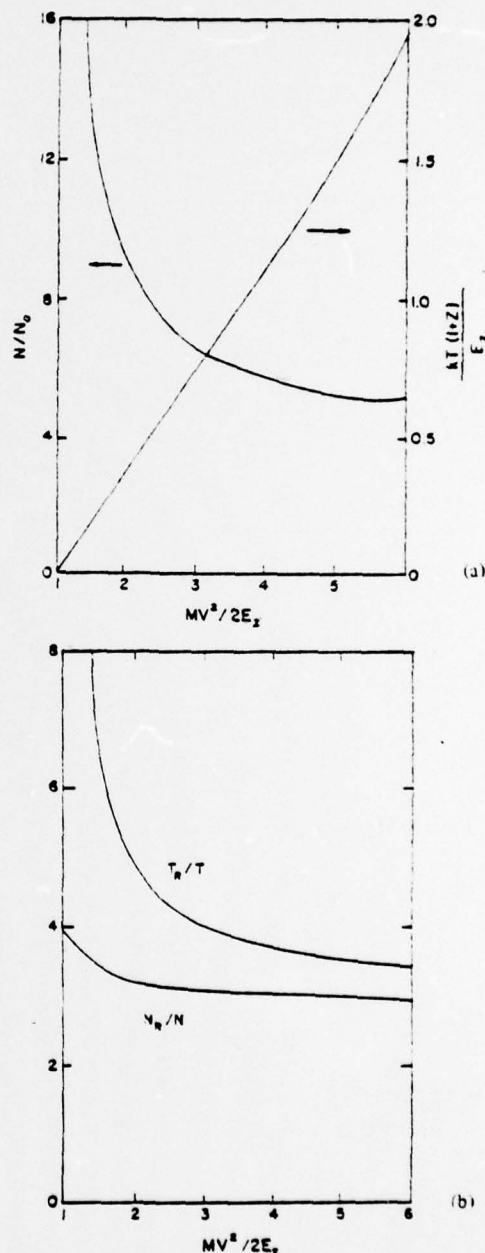compresses the gas by the factor N/N_0 which is also
shown in fig. 3(a).

Fig. 3. (a) The density and temperature behind the primary
shock wave as a function of the velocity of the primary shock
wave V. (b) The density and temperature behind the reflected
shock wave as a function of the velocity of the primary shock
wave V.

9

The conservation laws for the reflected shock wave are

$$N M (u + V_R) = N_R M V_R \qquad (6)$$

$$N M (u + V_R)^2 + P = N_R M V_R^2 + P_R, \qquad (7)$$

$$\tfrac{1}{2} M (u + V_R)^2 + H = \tfrac{1}{2} M V_R^2 + H_R, \qquad (8)$$

where V_R is the velocity of the reflected shock wave, and P_R and H_R are the pressure and enthalpy behind the reflected shock wave:

$$P_R = k T_R N_R (1 + Z), \qquad (9)$$

$$H_R = \tfrac{1}{2} k T_R (1 + Z) + E_z. \qquad (10)$$

After solving eqs. (6)–(8), the density and temperature behind the reflected shock wave are found to increase by factors of 3 to 4 as shown in fig. 3(b). The compression of the ambient gas by the primary and reflected shock waves is particularly important for elements with low vapor pressure such as lithium and beryllium. Additional compression may be achieved by tapering the end of the shock tube so that the shock wave comes to a focus [13,14].

The plasma behind the reflected shock wave expands through a nozzle and mixes with the gas target in the interaction region shown in fig. 1. The gas target may be confined behind a diaphragm which is burst as the plasma expands through the nozzle, or the gas may be injected into the plasma flow [15]. In the event the target gas pressure is so high as to prevent mixing, it may be necessary to mix by injection of the target gas in a manner similar to that widely used in chemical lasers. In this case the mixing time must be short and various fast mixing schemes will have to be investigated. During charge-exchange reactions between the fully stripped plasma ions and the neutral target atoms, electrons are picked up into excited states of the hydrogen-like plasma ion. At thermal energies, endothermic charge exchange reactions are negligible compared to near-resonant exothermic reactions [16]. Thus the target atom may be selected to direct the electron transfer into a specific excited state of the hydrogen-like ion. For example, the energy levels of Li III and xenon are shown in fig. 4. Charge transfer should be primarily into the $N = 3$ level of the lithium ion, with most of these electrons going into the highly degenerate 3D state. Thus, the upper state of the Balmer-α transition is preferentially filled. Landau-Zener calculations indicate that the charge exchange section is of order [4]

$$\sigma_p = 10^{-16} Z^2 \text{ cm}^2 \qquad (11)$$

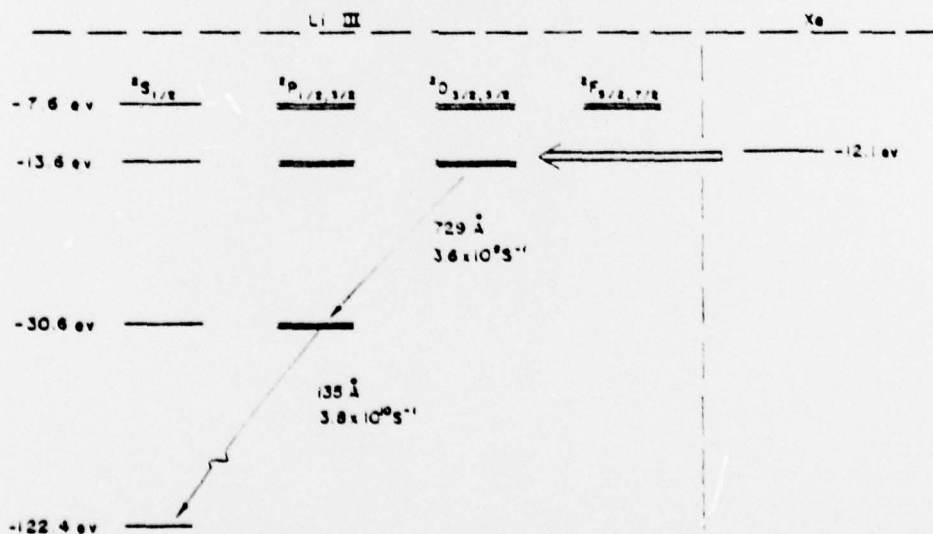

Fig. 4. Energy levels of hydrogen-like lithium and xenon, showing the nearly-resonant electron transfer pump reaction and the Balmer-α transition at 729 Å.

at thermal energies. The charge exchange rate is $\sigma_p V_z$. where V_z is the thermal velocity of the ion. Processes that compete with the charge exchange pump reaction such as electron impact ionization and excitation of the target atoms, must be alleviated. This may be done by reducing the average plasma electron energy to less than the ionization and excitation threshold of the target atom by allowing the plasma to expand rapidly through a nozzle. The expansion time must be smaller than R_r^{-1}. the time constant for recombination, so that the degree of ionization is "frozen" in a manner somewhat analogous to the "freezing" of vibrational energy in gas dynamic lasers [17].

3. Laser gain

The net linear gain may be written [18]

$$G = \lambda^2 A_u L \Delta V / 8\pi \Delta v - \sigma_{abs} N_\tau L. \qquad (12)$$

where σ_{abs} is the cross section for absorption of radiation with wavelength λ in the target gas. and N_τ is the density of target atoms. We neglect photoabsorption by the plasma ions and electrons. Taking into account the pumping rate $\sigma_p V_z N_\tau$. the collisional depopulation of the upper laser state C_u [10]. and spontaneous decay A_u. the steady-state population inversion is

$$\Delta V = \frac{\sigma_p V_z N_\tau N_z}{A_u + C_u} \quad (1 - A_u g_u / A_\ell g_\ell) \qquad (13)$$

where N_z is the density of fully stripped plasma ions. Since for the Balmer-α transition $A_u g_u \ll A_\ell g_\ell$, the gain is approximately

$$G = N_\tau L [\lambda^3 N_z \sigma_p / 4\pi^2 - \sigma_{abs}]. \qquad (14)$$

We have also assumed that the Doppler broadening of the spectral line is much greater than Stark broadening [19]. and that radiative decay of the upper laser state dominates collisional depopulation ($A_u > C_u$). This last assumption effectively puts an upper limit on the electron density in the interaction region. For positive gain to occur, we must have

$$N_z > 4\pi^2 \sigma_{abs} / \sigma_p \lambda^3. \qquad (15)$$

which puts a lower limit on the fully stripped ion den-

Table 1
Values for the photoabsorption cross section σ_{abs} are from refs. [20] and [21].

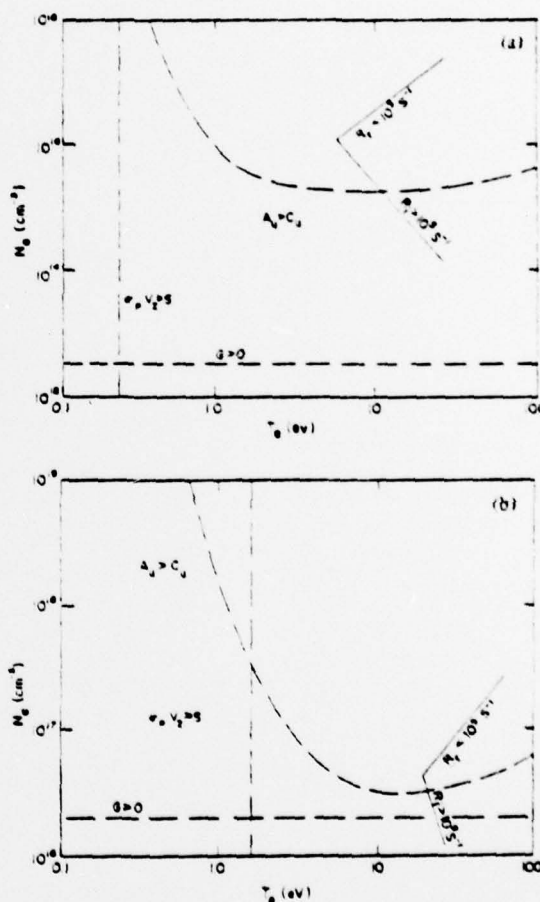|	$He^{2+} + Na$	$Li^{3+} + Xe$
λ (Å)	1640	729
A_u (s^{-1})	7.1×10^8	3.6×10^9
σ_p (cm^2)	4×10^{-16}	9×10^{-16}
σ_{abs} (cm^2)	7×10^{-20}	6×10^{-17}
N_z^{min} (cm^{-3})	2×10^{12}	7×10^{15}

Fig. 5. (a) Plasma parameters for formation of the fully stripped plasma (solid lines) and for lasing on the Balmer-α line of helium. (b) Plasma parameters for formation of the fully stripped plasma (solid lines) and for lasing on the Balmer-α line of lithium.

sity in the interaction region as given in table 1. Note that condition (15) is independent of the temperature in the interaction region. The upper and lower bounds on the electron density in the interaction region are shown in fig. 5, for the two cases of helium and lithium ions. The plasma parameters N_e and T_e necessary for formation of the fully stripped plasma are also shown in fig. 5. We require that the plasma formation time R_i^{-1} be smaller than $10 \mu s$, the formation time of a typical shock tube generated plasma, and that the recombination time R_r^{-1} be greater than $10 \mu s$ so that the ionization is frozen as the plasma expands through the nozzle into the interaction region. As mentioned above, the electrons must rapidly cool as the plasma expands through the nozzle. Then electron collisional ionization and excitation of the target atoms do not dominate the charge exchange pump reaction. This implies that

$$\sigma_p V_z N_z > N_e (S_{ion} + S_{exc}). \quad (16)$$

where S_{ion} and S_{exc} are the rates for electron impact ionization and excitation of the target atoms [22]. Condition (16) puts an upper bound on the electron temperature in the interaction region as given in table 2. Thus the electron temperature must decrease by about an order of magnitude as the plasma expands through the nozzle.

The net gain given by eq. (14) is a function of the densities N_z and N_π in the interaction region and the length L of the active region. Taking the densities equal to 3×10^{16} cm^{-3} and L equal to 10 cm, the

Table 2
Ionization is designated I and excitation E. The threshold energy is E_0, and Q_0 is the maximum cross section.

Reactant		Q_0 (cm^2)	E_0 (eV)	T_e^{max} (eV)
Na	I	8.5×10^{-16}	5.1	0.7
	E	2.2×10^{-15}	2.1	0.3
Xe	I	5.3×10^{-16}	12.1	2.1
	E	1.6×10^{-17}	3.7	1.6

gain is 400 for the Balmer-α line of helium (1640 Å) and 60 for lithium (729Å)

References

[1] J.W. McGowan and R.F. Stebbings, Appl. Opt. Suppl. 2 (1965) 68.
[2] B.M. Smirnov, JETP Lett. 6 (1967) 78.
[3] L.P. Presnyakov and V.P. Shevel'ko, JETP Lett. 13 (1971) 203.
[4] A.V. Vinogradov and I.I. Sobel'man. Sov. Phys. JETP 36 (1973) 1115.
[5] M.O. Scully, W.H. Louisell and W.B. McKnight, Opt. Commun. 9 (1973) 246.
[6] R.C. Elton, in Progress in Lasers and Laser Fusion, eds. B. Kursonoglu, A. Perlmutter and S. Widmayer (Plenum, New York, 1975), p. 117.
[7] D. Anderson, J. McCullen, M.O. Scully and J.F. Seely, Opt. Commun. 17 (1976) 226.
[8] D.A. Copeland and C.L. Tang, Opt. Commun. 18 (1976) 155.
[9] J.F. Seely, J. Appl. Phys. (to be published).
[10] H.R. Griem, Plasma Spectroscopy (McGraw-Hill, New York, 1964), p. 129–168.
[11] A.C. Kolb and H.R. Griem, in Atomic and Molecular Processes, ed. D.R. Bates (Academic Press, New York, 1962) p. 141.
[12] R.C. Elton and H.R. Griem, Phys. Rev. 135 (1964) 1550.
[13] V.A. Belokon, A.I. Petrukhin and V.A. Proskuryakov, Sov. Phys. JETP 21 (1965) 33.
[14] B.E. Milton and R.D. Archer, in Shock Tube Research, eds. J.L. Stollery, A.G. Gaydon and P.R. Owen (Chapman and Hall, London, 1971).
[15] A.S. Bashkin et al., Sov. J. Quant. Electron. 6 (1976) 256.
[16] H.J. Zwally and P.G. Cable, Phys. Rev. A4 (1971) 2301.
[17] E.T. Gerry, AIAA Paper No. 71–23 (1971), American Institute of Aeronautics and Astronautics, New York.
[18] A. Yariv, Quantum electronics (Wiley, New York, 1975), p. 162.
[19] H.R. Griem, Broadening of Spectral Lines by Charged Particles in Plasmas (Academic Press, New York, 1974) p. 279.
[20] R.E. Huffman, Y. Tanaka and J.C. Larrabee, J. Chem. Phys. 39 (1963) 902.
[21] G.V. Marr and D.M. Creek, Proc. Roy. Soc. A 304 (1968) 233.
[22] M. Mitchner and C.H. Kruger, Partially ionized gases (Wiley – Interscience, New York, 1973) p. 43.

Soft x-ray laser pumped by charge exchange between C VII and Ar III in expanding laser-produced plasma[a]

John F. Seely[b] and William B. McKnight

Department of Physics, The University of Alabama in Huntsville, Huntsville, Alabama 35807
(Received 21 February 1977; accepted for publication 17 May 1977)

A soft x-ray laser with wavelength 182 Å is proposed. The pumping mechanism is charge exchange between C VII and Ar III which occurs when a laser-produced carbon plasma expands into an argon background gas. Electron pickup is primarily into the $n = 3$ level of C VI, and the laser transition is the Balmer-α line. Nd-glass radiation is converted into 182 Å radiation with efficiency of order 1%.

I. INTRODUCTION

Due to the unfavorable scaling of small-signal laser gain with wavelength, λ^3 in the case of Doppler broadening, a large population inversion must be generated in order to demonstrate lasing below 1000 Å.[1] In addition, pumping of the upper laser state must be rapid to overcome the spontaneous decay of the laser transition. The requirements of high density and rapid pumping are satisfied in laser-produced plasmas. Suggested pumping mechanisms are recombination into high-lying energy states,[2] electron collisional excitation,[3] photoionization,[4] and charge exchange.[5] Of these, charge exchange seems to be the most promising at the present time.[1]

In this paper, we shall consider the conditions under which lasing on the Balmer-α line of hydrogenlike carbon may occur when a laser-produced carbon plasma expands into a background gas. The pumping mechanism is the charge exchange reaction

$$C^{-6} + Y^{-i} \rightarrow C^{-5}(n) + Y^{-(i-1)}, \qquad (1)$$
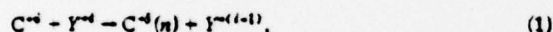
where Y^{-i} is the background species with charge i, and n is the excited energy level of the hydrogenlike carbon

ion. We are particularly interested in the Balmer-α transition $n = 3 \rightarrow 2$ at 182 Å, since this is the shortest-wavelength $\Delta n = 1$ transition and does not terminate on the ground level of the ion. Carbon plasmas produced from graphite and polyethylene targets have been widely studied,[4] and we shall limit our discussion to this element. The scheme could be extended to include other solid targets, as well as plasmas formed from gaseous targets.

Elton and Dixon[5] have suggested neutral helium as a candidate for the background gas reactant. As we show below, it is unlikely that neutral atoms will survive in the environment of intense radiation and hot electrons near the solid target. We propose that an ionized species, such as Ar III, be used instead.

The configuration is shown in Fig. 1. Neodymium-glass laser radiation of intensity 10^{11}–10^{12} W/cm^2 is focused on a solid graphite or polyethylene target
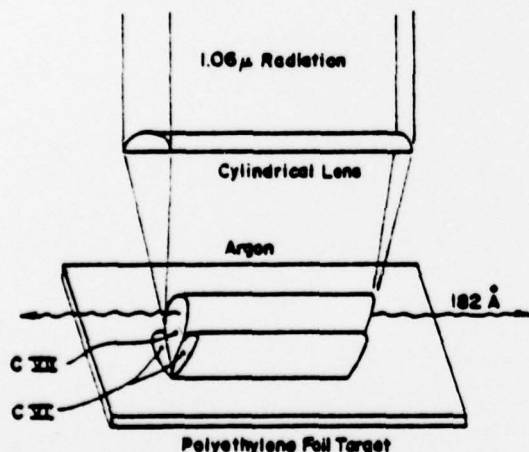

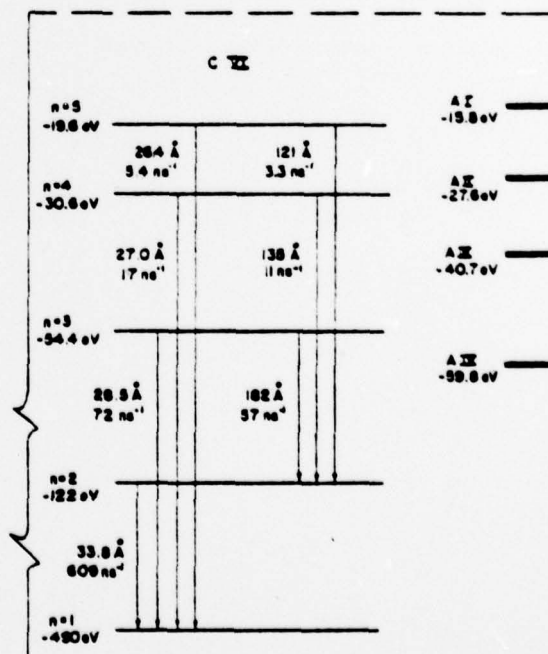FIG. 1. The experimental configuration for a C VII/Ar III 182-Å laser.

FIG. 2. Energy levels of C VI and ionization potentials of argon.


TABLE I. Temperatures and densities at distance x from the target (Ref. 11).

x (mm)	T_e (eV)	N_e (10^{19} cm^{-3})	N_c (10^{17} cm^{-3})
1.0	39	4	2
1.6	17	0.9	0.3
2.3	9	0.17	0.08

immersed in a background gas such as argon. The background gas must be at low pressure so that breakdown does not occur. A dense carbon plasma expands into the background gas. Plasma electrons and continuum radiation rapidly ionize the background atoms near the plasma-gas interface. As we show below, the charge exchange reaction

$$C^{+6} + Ar^{+2} \rightarrow C^{+5}(n=3) + Ar^{+3} \qquad (2)$$
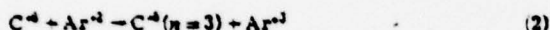
is more rapid than the electron collisional ionization of Ar III. This charge exchange reaction preferentially fills the $n=3$ level of C VI (see Fig. 2), and lasing on the 182-Å line of C VI may occur along the plasma-gas interface.

II. PLASMA FORMATION

A dense carbon plasma may be readily formed by focusing intense laser radiation on graphite or polyethylene solid targets or a methane gaseous target. We shall limit our consideration to plasma formed from a polyethylene foil target, since this has been most extensively studied.[1-13]

When Q-switched ruby or Nd-glass radiation with intensity 3×10^{11} W/cm^2 is focused onto a polyethylene foil 0.25 mm thick, a dense carbon plasma is formed at the foil surface.[1-12] The plasma expands adiabatically as electron thermal energy is converted into streaming motion of the ions. For ideal spherical expansion, the plasma density decreases as x^{-3} and the electron temperature as x^{-2}. The measured electron densities and temperatures at various distances from the foil are given in Table I. At distances greater than 1 mm, the ions stream outward with velocity 3×10^7 cm/sec. About 70% of the incident laser energy is converted into ion streaming energy.

The plasma from the polyethylene (C_2H_4)$_n$ foil is composed of highly ionized carbon and hydrogen. The highest ionization state C VII expands preferentially in the direction normal to the target surface, and the lower ionization states, including hydrogen,[8] are directed more parallel to the target surface. The C VII ions are also concentrated at the leading edge of the expanding plasma.[9] Thus, the short-wavelength laser species C VII is separated from the bulk of the plasma in both space and time as shown in Fig. 1, and is available to feed the laser pump reaction (2) at the plasma-gas interface. This is in contrast to C VI, the laser species of Ref. 7, which is concentrated in the interior of the plasma.

The experiments described in Refs. 8—12 were performed in a vacuum. If the polyethylene target is immersed in argon, we must ensure that the argon

background gas does not break down and absorb the 1.06-μ radiation, thereby preventing formation of the carbon plasma. The experimentally observed[14-16] intensity thresholds for breakdown of argon by Q-switched Nd-glass radiation are shown in Fig. 3. The breakdown threshold increases sharply as the argon pressure, lens focal length, and pulse duration are reduced. The breakdown threshold should be well above 3×10^{11} W/cm^2 for argon pressure below 100 Torr, focal length of several centimeters, and pulse duration of 10 nsec. We note that the breakdown thresholds for picosecond pulses[17] are two orders of magnitude higher than those shown in Fig. 3, but it is uncertain that a large number of carbon ions would be fully stripped in a pulse of such short duration. The breakdown threshold for CO_2 laser radiation is more than an order of magnitude lower[18] than those of Fig. 3.

Breakdown effects place an upper limit of about 100 Torr on the argon pressure near the surface of the polyethylene foil. As we show in Sec. III, absorption of 182-Å radiation puts an even more severe limit on the argon pressure.

An alternate arrangement would be to let the plasma formed in a vacuum expand through a slit into a chamber containing higher-pressure argon.[19] But the plasma density would decrease during the expansion, resulting in lower laser gain, and the gas pumping requirements would be a cumbersome experimental restraint.

For a target immersed in a background gas of pressure 1—10 Torr, the initial expansion of the carbon plasma is not affected by the presence of the background gas.[20] But after 100 nsec, when the plasma has expanded to a radius of several millimeters, a blast wave separates from the leading edge of the plasma and propagates ahead of the plasma-gas interface.[20-22] The gas behind this shock wave is highly ionized.[20] We show below that formation of the population inversion and lasing on the 182-Å line of C VI should occur within a
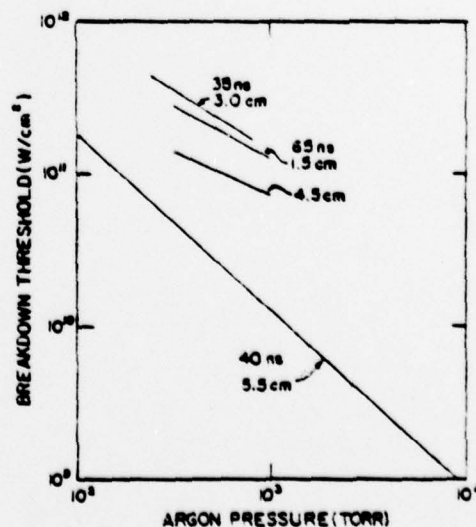

FIG. 3. Intensity threshold for breakdown of argon by Q-switched Nd-glass radiation (Refs. 14—16).
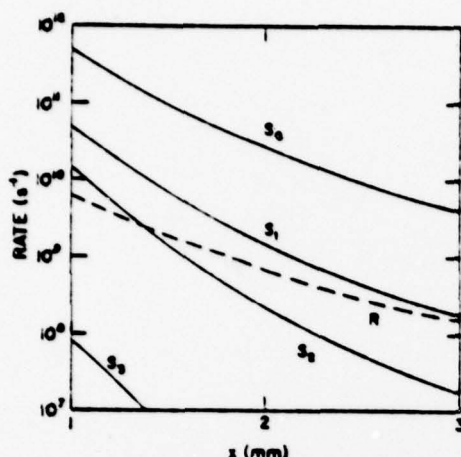
FIG. 4. Rates of electron collisional ionization of argon S and charge exchange R.

millimeter of the target surface before development of the blast wave occurs.

The carbon plasma, expanding into the argon background gas, forms the active medium of the 182-Å laser. In order to ensure that lasing occurs along the axis of the active medium, the length of the active medium must be much greater than the transverse dimension. For example, assume that a 1-cm-diam beam of Nd-glass radiation is focused by a cylindrical lens to a rectangular spot of length 1 cm and width 100 μ on the polyethylene foil. For pulse duration 10 nsec and focused intensity 3×10^{11} W/cm^2, the Nd-glass laser energy must be 30 J. At a distance of 1 mm from the foil, the transverse dimension of the plasma has expanded to about 1 mm.[3] The C VII ions interact with the argon background gas over an area about 1 cm long and 1 mm wide, and lasing should occur along the 1-cm length of the plasma. If 70%[3] of the Nd-glass radiation energy is converted into C VII with streaming velocity 3×10^7 cm/sec (kinetic energy 5.6 keV), the total number of ions produced is about 2×10^{16}. If each of these ions results in the emission of a 182-Å photon, the total energy emitted is 0.2 J. Thus an upper bound on the efficiency of conversion of 1.06 μ radiation to 182-Å radiation is approximately 1%.

III. COLLISIONAL PROCESSES

At the interface between the expanding carbon plasma and the argon background gas, argon atoms are rapidly ionized by electron collisions. For Maxwellian electron distribution with temperature T_e, the rate of electron collisional ionization is[23]

$$S_i = N_e V_e \int_0^\infty \xi \exp(-\xi) \sigma_i \, d\xi, \qquad (3)$$

where $i = 0, 1, 2, \cdots$ is the argon charge state, σ_i is the cross section as a function of electron energy, and V_e is the average electron thermal velocity:

$$V_e = (8kT_e/\pi m_e)^{1/2}. \qquad (4)$$

The electron drift velocity is negligible compared to the

electron thermal velocity for the first few millimeters of plasma expansion. Using cross-section data[24] and the experimentally observed electron temperature and density near the polyethylene foil, the rate of electron collisional ionization of argon as a function of distance from the foil is shown in Fig. 4. It is apparent that ionization of the argon background gas by the plasma electrons is very rapid near the target.

Little theoretical or experimental work has been done on charge exchange reactions, such as reaction (2), involving two colliding ions. A Landau-Zener calculation extending the theory of Ref. 25 is in progress and will be reported elsewhere. Preliminary results indicate that the cross section for electron pickup into the $n = 3$ level of C VI is of the order of 10^{-15} cm^2, and pickup into other levels is smaller by an order of magnitude. Since the ion thermal velocity is negligible compared to the ion streaming velocity 3×10^7 cm/sec, the charge exchange rate is of the order of

$$R = (3 \times 10^{-8} \text{ cm}^3/\text{sec})N_c, \qquad (5)$$

where N_c is the density of C VII. Using the experimentally observed densities, the charge exchange rate as a function of distance from the polyethylene foil is given by the dotted line in Fig. 4. The two-electron transfer reaction

$$C^{+6} + Ar^{+2} \rightarrow C^{+4} + Ar^{+4} \qquad (6)$$
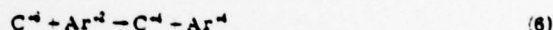
is exothermic by more than 700 eV and is negligible compared to single-electron transfer.[26]

In ideal adiabatic expansion, the electron density decreases as x^{-3} and the electron temperature as x^{-2}. The ionization rate given by Eq. (3) is proportional to $N_e T_e^{1/2}$, which decreases as x^{-4}. The charge exchange rate given by Eq. (5) decreases as x^{-3}. At distances less than 1.5 mm from the target, Ar III is more likely to undergo electron collisional ionization than the charge exchange reaction (2). Beyond 1.5 mm, the charge exchange reaction dominates.

The dense hot plasma near the surface of the foil target is a strong source of continuum radiation with wavelength greater than 500 Å.[3] From 400 Å to the ionization edge at 787 Å, the photoabsorption cross section of argon is 3×10^{-17} cm^2.[27] For argon pressure above 10 Torr, the ionizing continuum radiation is absorbed in the first millimeter of argon.

The argon gas near the target is rapidly ionized by the plasma electrons and continuum radiation. At distances of 1.5 mm or more from the target, the charge exchange reaction (2) dominates over electron collisional ionization. This is the region of interest for achieving a population inversion on the 182-Å line of C VI.

IV. THRESHOLD INVERSION

Due to low mirror reflectivity at 182 Å, sufficient population inversion must probably be generated for amplification to occur during a single pass through the laser medium. We shall calculate the population inversion that results in a single-pass gain of 10 cm^{-1} over a distance of 1 cm.

TABLE II. Argon ionization cross sections at threshold.

	Cross sections at threshold (Mb)		
	σ_i	Q_i	Q_i^a
Ar II	30	2	3
Ar III	10	0.9	1
Ar IV	< 0.1	.01	0.09

Recent progress has been made on multilayer reflective coatings in the vacuum ultraviolet. Reflectivity of 2.7% has been experimentally demonstrated at 182 Å, and higher reflectivities in the near future are likely.[28] It is shown below that use of 2.7% mirrors reduces the threshold gain by a factor of only 3, and it is doubtful that these multilayer coatings could withstand the high-intensity radiation generated when threshold is exceeded.

The threshold inversion may be written[29]

$$\Delta N_T = (8\pi/\lambda^2 A_{32} g)(10/L + L_a^{-1}), \tag{7}$$

where λ is the laser wavelength, A_{32} is the spontaneous transition rate, g is the linewidth, L is the laser length, and L_a is the loss length. The photoabsorption cross section for 182-Å radiation in neutral argon is[27]

$$Q_0 = 1.3 \times 10^{-18} \text{ cm}^2. \tag{8}$$

The absorption length in 10 Torr argon is 1.9 cm. If longer absorption lengths are required, as in a grazing incidence spectrometer, argon must be pumped to lower pressures, or the spectrometer must be filled with a low-absorption gas such as H_2 ($Q_0 = 1.6 \times 10^{-19}$ cm² [27]).

The photoabsorption cross sections of argon ions have not been measured. The photoabsorption cross section at ionization threshold may be estimated from the electron collisional cross section at threshold[30]

$$Q_i = \sqrt{3} \alpha I \sigma_i / \bar{g}, \tag{9}$$

where α is the fine structure constant, I is the ionization potential in atomic units, σ_i is the electron collisional cross section at threshold, and the effective Gaunt factor is $\bar{g} = 0.2$. The values of Q_i are listed in Table II. An independent estimate of the photoabsorption cross section may be obtained by treating the argon ion as a hydrogenlike ion with nuclear charge $(Z-1)$ [31]:

$$Q_i^a = 2^6 \pi^4 e^{10} m_e Z^4 / 3\sqrt{3} ch^6 n^3 \nu^3, \tag{10}$$

where n is the energy level and ν is the radiation frequency. This expression may be rewritten

$$Q_i^a = (2^6 \alpha \pi a_0^2 n/3\sqrt{3} Z^2)[Z^2 E_h / h\nu n^2]^3, \tag{11}$$

where E_h is equal to 13.6 eV. At ionization threshold, the quantity in square brackets is unity. Letting $n = (Z^2/2I)^{1/2}$, the values of Q_i^a at ionization threshold are given in Table II. The values of the photoabsorption cross sections of argon ions at ionization threshold estimated from Eqs. (9) and (11) agree fairly well. According to Eq. (11), the cross section at 182 Å is lower than the cross section at the ionization threshold by the factor $(182 \text{ Å}/\lambda_i)^3$, where λ_i is the wavelength at the ionization threshold. The photoabsorption of 182 Å in ionized argon is thus less than 10^{-18} cm². Free-free

absorption, Thomson scattering, and diffraction losses are negligible compared to photoabsorption.

Returning to Eq. (7), the dominant loss mechanism for the 182-Å laser radiation is photoabsorption by the ionized argon near the plasma-gas interface. For argon pressure of 10 Torr, the loss term L_a^{-1} is less than 0.4 cm⁻¹. For laser length 1 cm,

$$(10/L + L_a^{-1}) = 10.4 \text{ cm}^{-1}. \tag{12}$$

We note that if 2.7% mirrors were used, this factor becomes

$$(\ln R^{-2}/2L + L_a^{-1}) = 4.0 \text{ cm}^{-1}, \tag{13}$$

which reduces the threshold inversion (7) by a factor of about 3.

The spectral broadening of several of the $\Delta n = 1$ transitions of C VI at a distance of 1 mm from the foil have been measured[10] and are shown in Table III. The dominant broadening mechanism for these lines is Stark broadening due to quasistatic ion-ion collisions. Scaling from the 5290-Å line, the full Stark width at half-maximum goes like[10]

$$\Delta\lambda = (33 \text{ Å})(\lambda/5290 \text{ Å})^2 (n_i/7), \tag{14}$$

where n_i is the lower energy level. These scaled Stark widths are also given in Table III. The plasma expansion velocity normal to the foil surface is 3×10^6 cm/sec. The component of velocity in the direction parallel to the foil surface is an order of magnitude smaller.[12] The ion thermal velocity is negligible compared to the expansion velocity. The full Doppler widths due to the component of the expansion velocity parallel to the foil surface are given in the last column of Table III. It is apparent that the 182-Å line is primarily Doppler broadened. The linewidth

$$g^{-1} = (\Delta\lambda c/\lambda^2)(\tfrac{1}{4}\pi \ln 2)^{1/2} \tag{15}$$

is equal to 3.4×10^{12} sec⁻¹.

The fine structure states of a given level n of a hydrogenlike ion are rapidly mixed by electron collisions. If the mixing rate is faster than the radiative decay rate of the level n, then the fine structure states are occupied according to their statistical weights. The condition for statistical equilibrium is[32]

$$N_e/T_e^{1/2} \geq (6 \times 10^6 \text{ sec}) A_{np}/n^4, \tag{16}$$

where A_{np} is the radiative decay rate of the np state,

TABLE III. Spectral broadening of the $\Delta n = 1$ transitions of C VI.

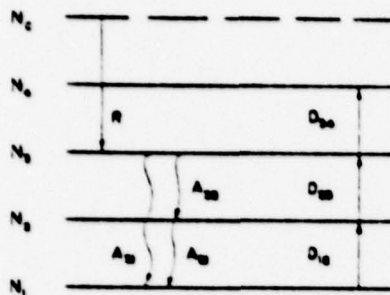| n_u	n_l	λ (Å)	$\Delta\lambda$ (Å) full width at half-maximum		
			Stark (observed)	Stark (scaled)	Doppler
9	7	5290	33	33	1.1
7	6	3434	13	12	0.69
6	5	2070	4	3.6	0.41
5	4	1125		0.95	0.23
4	3	521		0.14	0.10
3	2	182		0.01	0.036
2	1	34		0.0002	0.0068

FIG. 3. Transitions included in the rate equations for the populations of the levels of C VI.

N_e is the plasma electron density in units of cm^{-3}, and T_e is the electron temperature in units of eV. For C VI, $A_{10} = 2.2 \times 10^{11} \ sec^{-1}$ and condition (16) is well satisfied in dense laser-produced plasmas. The transition probabilities for C VI shown in Fig. 2 are scaled from hydrogen assuming statistical occupation of the fine structure states.[33] The radiative transition rate for the 182-Å line is

$$A_{32} = 5.7 \times 10^{10} \ sec^{-1}. \qquad (17)$$

Substituting Eqs. (12), (15), and (17) into Eq. (7), the threshold inversion is

$$\Delta N_T = 4.7 \times 10^{15} \ cm^{-3}. \qquad (18)$$

This is more than an order of magnitude lower than the density of C VII in the plasma 1—2 mm from the foil target.

V. RATE EQUATIONS

The interaction of an expanding plasma with a background gas is a difficult problem to model. We shall limit our consideration to distances greater than 1.3 mm from the target where gain on the 182-Å line of C VI is most likely to occur. At these distances, the argon background gas is twice ionized by the plasma electrons, and the laser pump reaction (2) dominates over further ionization of the argon ions.

The electron densities and temperatures of laser-produced plasmas are in the corona equilibrium regime. The population of the lower excited states of C VI are determined by collision-induced upward transitions and spontaneous downward transitions, as shown in Fig. 5. Here A_{nm} is the spontaneous decay rate given in Fig. 2, and D_{nm} is the collisional excitation rate[31]

$$D_{nm} = (4.5 \times 10^{-6} \ sec^{-1})N_e f_{nm}[\Delta E T_e^{1/2} \exp(\Delta E/T_e)]^{-1}, \qquad (19)$$

where N_e is the electron density in units of cm^{-3}, T_e is the temperature in eV, ΔE is the energy gap in eV, and f_{nm} is the oscillator strength.

The laser-produced carbon plasma is optically thick to Lyman-α radiation in the dense region near the polyethylene foil surface,[34] but is optically thin at distances greater than 2 mm from the foil surface[11] where the laser under consideration is expected to operate; consequently, radiation trapping of Lyman radiation

may be neglected. The electron-ion recombination rate is of the order of $10^5 \ sec^{-1}$,[11] and is small compared to the charge exchange rate R given by Eq. (5). We note that population inversions due to electron-ion recombination in a laser-produced carbon plasma have been experimentally observed.[12] However, the population inversions are so low that demonstration of significant laser gain may require traveling-wave excitation. The charge exchange rate given by Eq. (5) is two orders of magnitude larger than the recombination rate, and should lead to much larger population inversions.

The population inversion for the $n = 3 \rightarrow 2$ transition is

$$\Delta N = N_3 - g_3 N_2 / g_2, \qquad (20)$$

where $g_n = 2n^2$ is the degeneracy of the nth level. In steady state, the rate equations for the upper laser state N_3 and the lower laser state N_2 reduce to

$$(A_{31} + A_{32} + D_{34})N_3 = RN_{III} + D_{23}N_2, \qquad (21)$$

$$(A_{21} + D_{23})N_2 = A_{32}N_3 + D_{12}N_1, \qquad (22)$$

where N_{III} is the density of Ar III. The steady-state population inversion may be written

$$\Delta N = \frac{(RN_{III} + D_{23}N_2)(1 - 9A_{32}/4A_{21})}{(A_{31} + A_{32} + D_{34})} - \frac{9D_{12}N_1}{4A_{21}} \qquad (23)$$

Due to the large energy gap between the $n = 1$ and 2 levels, D_{12} is about seven orders of magnitude smaller than A_{21}, and the last term in Eq. (23) is negligible. If radiation trapping of the 33.8-Å Lyman-α radiation were important, this term would be larger. The term $D_{23}N_2$ in Eq. (23) is negligible compared to RN_{III}.
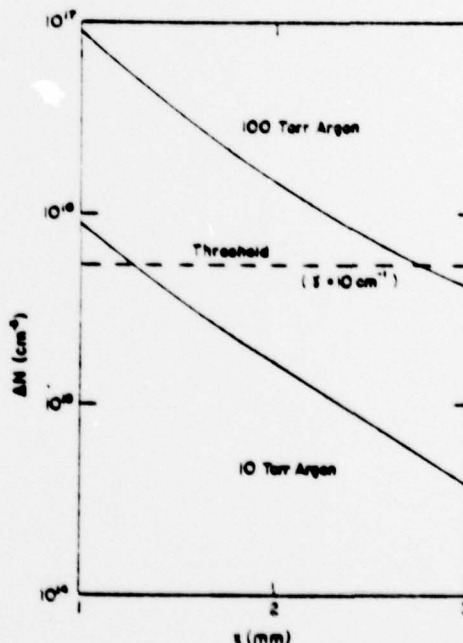
Using Eqs. (5) and (19) and the spontaneous transi-

FIG. 6. Population inversions for the 182-Å transition of C VI at argon pressures of 10 and 100 Torr.

3695   J. Appl. Phys., Vol. 48, No. 9, September 1977

J.F. Seely and W.B. McKnight   3695

tion probabilities listed in Fig. 2, the population inversion is

$$\Delta N = \frac{(1.3\times10^{-19})N_v V_{111}}{[1 - 1.2\times10^{-11}N_e {}^{2} z_i {}^{7/2} \exp(-23.3/T_e)]} , \quad (24)$$

where the densities are in units of cm^{-3} and the electron temperature is in units of eV. Using the densities and temperatures listed in Table I, the population inversion is shown in Fig. 6. Background gas pressures of 10—100 Torr are needed to achieve threshold inversion at distances of 1—2 mm from the foil surface.

[1] R.W. Waynant and R.C. Elton, Proc. IEEE 64, 1059 (1976).
[2] G.J. Pert and S.A. Ramsden, Opt. Commun. 11, 270 (1974); W.W. Jones and A.W. Ali, Appl. Phys. Lett. 26, 450 (1975); R.A. Andrews in *Progress in Lasers and Laser Fusion*, edited by A. Perlmutter and S.W. Widmayer (Plenum, New York, 1975), p. 235; R.C. Elton, Appl. Opt. 14, 97 (1975); J. Davis and K.G. Whitney, Appl. Phys. Lett. 29, 419 (1976).
[3] R.C. Elton, Appl. Opt. 14, 2243 (1975).
[4] M.O. Scully, W.H. Louisell, and W.B. McKnight, Opt. Commun. 9, 246 (1973); A.V. Vinogradov and I.I. Sobel'man, Sov. Phys.-JETP 36, 1115 (1973).
[5] T.P. Hughes, *Plasmas and Laser Light* (Wiley, New York, 1975).
[6] R.C. Elton and R.H. Dixon, in *Proc. Int. Conf. on Beam-Foil Spectroscopy*, edited by I.A. Sellin and D.J. Pegg (Plenum, New York, 1976), Vol. 2, p. 973.
[7] B.C. Boland, F.E. Irons, and R.W.P. McWhirter, J. Phys. B 1, 1180 (1968).
[8] F.E. Irons, R.W.P. McWhirter, and N.J. Peacock, J. Phys. B 5, 1975 (1972).
[9] F.E. Irons, J. Phys. B 6, 1562 (1973).
[10] F.E. Irons and N.J. Peacock, J. Phys. B 7, 2084 (1974).
[11] F.E. Irons and N.J. Peacock, J. Phys. B 7, 1109 (1974); R.J. Dewhurst, J. Jacoby, G.J. Pert, and S.A. Ramsden, Phys. Rev. Lett. 37, 1265 (1976).
[12] F.E. Irons, J. Phys. B 8, 3044 (1975).
[13] R.G. Tomlinson, E.K. Damon, and H.T. Busher in *Physics of Quantum Electronics*, edited by P.L. Kelly, B. Lax, and P.T. Tannenwald (McGraw-Hill, New York, 1966), p. 520.
[14] V.E. Mitsuk and V.A. Cherikov, JETP Lett. 6, 124 (1967).
[15] T. Bergquist and B. Kleman, Ark. Fys. 31, 177 (1966).
[16] C.L.M. Ireland and C. Grey Morgan, J. Phys. D 7, L87 (1974).
[17] C.H. Chan, C.D. Moody, and W.B. McKnight, J. Appl. Phys. 44, 1179 (1973).
[18] Wayne Ehler, Phys. Fluids 16, 339 (1973).
[19] N.G. Basov, V.A. Gribkov, O.N. Krokhin, and G.V. Sklizkov, Sov. Phys.-JETP 27, 575 (1968).
[20] D.C. Emmony and J. Irving, J. Phys. D 2, 1186 (1969).
[21] R.B. Hall, J. Appl. Phys. 40, 1941 (1969).
[22] M. Mitchner and C.H. Kruger, *Partially Ionized Gases* (Wiley, New York, 1973), p. 43.
[23] W. Bleakney, Phys. Rev. 36, 1303 (1930).
[24] L.P. Preshyakov and A.D. Ulantsev, Sov. J. Quantum Electron. 4, 1320 (1975).
[25] J. Goldhar, R. Mariella, and A. Javan, Appl. Phys. Lett. 29, 96 (1976).
[26] J.A.R. Samson, in *Advances in Atomic and Molecular Physics*, edited by D.R. Bates and I. Estermann (Academic, New York, 1966), Vol. 2, p. 199.
[27] R.-P. Haelbich and C. Kunz, Opt. Commun. 17, 287 (1976).
[28] Amnon Yariv, *Quantum Electronics* (Wiley, New York, 1975).
[29] M.J. Seaton, in *Atomic and Molecular Processes*, edited by D.R. Bates (Academic, New York, 1962), p. 416.
[30] H. Griem, *Plasma Spectroscopy* (McGraw-Hill, New York, 1964).
[31] E. Hinnov and F.W. Hofmann, J. Opt. Soc. Am. 53, 1259 (1963).
[32] W.L. Wiese, M.W. Smith, and B.M. Glennon, *Atomic Transition Probabilities* (National Bureau of Standards, Washington, D.C., 1966), Vol. 1.
[33] B.A. Norton and N.J. Peacock, J. Phys. B 8, 989 (1975).